Vibrational Spectroscopy 75 (2014) 169–172

Contents lists available at ScienceDirect

Vibrational Spectroscopy

journal homepage: www.elsevier.com/locate/vibspec

3D FT-IR imaging spectroscopy of phase-separation in a poly(3-hydroxybutyrate)/poly(L-lactic acid) blend*

Miriam Unger[a,b], Julia Sedlmair[c], Heinz W. Siesler[d], Carol Hirschmugl[a,*]

[a] Department of Physics, University of Wisconsin-Milwaukee, Milwaukee, WI 53211. USA
[b] Cetics Healthcare Technologies GmbH, D 73728 Esslingen a. N.. Germany
[c] Forest Products Laboratory, US Department of Agriculture Forest Service, Madison, WI 53726. USA
[d] Department of Physical Chemistry. University of Duisburg-Essen, D 451 17 Essen, Germany

ARTICLE INFO

Article history:
Available online 6 August 2014

Keywords:
3D FT-IR imaging spectroscopy
Poly-(3-hydroxybutyrate)/poly(L-lactic acid) blend
Phase separation
3D blend morphology

ABSTRACT

In the present study, 3D FT-IR spectroscopic imaging measurements were applied to study the phase separation of a poly(3-hydroxybutyrate) (PHB)/poly(L-lactic acid) (PLA) (50:50 wt.%) polymer blend film. While in 2D projection imaging the z-dependent information is overlapped, thereby complicating the analysis, FT-IR spectro-micro-tomography, obtained from computed tomographic back projection calculations, results in distinct 3D chemical images that provide detailed information of phase separation of the two polymer components that are well separated.

1. Introduction

Generally, one of the goals of studying polymer blends has been to enhance their useful attributes and to eliminate the deleterious properties of the individual components. There have also been investigations aimed at generating an understanding of the fundamental nature of polymer mixtures. Unfortunately, most pairs of chemically different polymers are mutually immiscible and mixing usually results in materials that are phase-separated and have weak polymer–polymerinteractions/interfaces [1,2]. The mixing properties of polymers are generally discussed by considering the changes in the Gibbs free energy. Moreover, it is also known that the miscibility of different polymers depends on their concentration, the temperature and their chemical structures. By considering the composition dependence of the free energy of mixing, a phase diagram can be constructed to characterize the phase behavior of the mixture. Further information on the thermodynamics of polymer blends taking into account their miscibility is described in detail elsewhere [3–5]. In this context, a phase-separated poly(3-hydroxybutyrate) (PHB)/poly(L-lacticacid) (PLA) (50:50wt.%) polymer blend film (Fig. 1) has been analyzed by 3D FT-IRimaging spectroscopy.

Contrary to the conservative 2D imaging technique this analytical approach offers the possibility to combine spectral and spatial information by measuring several hundred thousand spectra of laterally resolved sample positions during 360° rotation ofthe sample in a relatively short time thereby providing "chemical images" of the three-dimensional blend morphology [6–10].This is feasible with the Synchrotron based IRENI beamline [11] optimized for widefield microspectroscopy.IRENI extracts 320 mrad horizontal synchrotron radiation from a bending magnet, separates the light into 12 beamlets that are recombined with optics to homogeneously illuminate a 140 μm × 140 μm area and refocused onto 128 × 128 pixel focal plane array detector. Due to the high brightness of the source and employing the multi-element pixelated detector, spatially resolved 2D projection data are rapidly collected for tomography experiments.

Poly(3-hydroxybutyrate) (PHB) [12-14] is a thermoplastic polyester,with great commercialpotential because it can be biologically synthesized from renewable sources and it is biodegradable. Despite these outstanding characteristics, the applications of this polymer are limited, due to its high crystallinity, its crystalline phase morphology and the secondary crystallization that occurs after processing, which leads to a material with poor mechanical properties. Another restriction of this material is the thermal instability above the melting point, around 174°C. One method to improve the properties of this material is to prepare blends with other polymers, which is a relatively fast and inexpensive

* Paper presented at the 7th International Workshop on Infrared Microscopy and Spectroscopy with Accelerator-BasedSources (WIRMS). Melbourne, Australia, 10–13th November 2014.

* Corresponding author. Tel.: +1414 229 5748; fax: +1414 229 5589.
E-mail addresses: cjhirsch@uwm.edu.cjhirsch@uwm.com (C. Hirschmugl).

http://dx.doi.org/10.1016/j.vlbspec.2014.07.007
0924-2031/

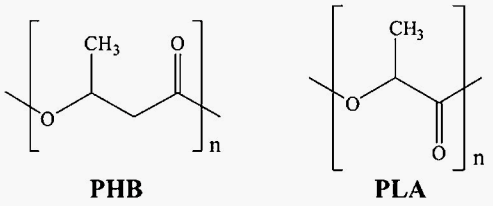

Fig. 1. Chemical structures of PHB and PLA repetition units.

option. Poly(L-lactic acid) (PLA) [15-17] can be produced by polycondensation of lactic acid or by ring-opening polymerization of the cyclic lactide dimer. The monomeric raw material can be obtained from renewable agricultural sources such as corn. PLA is already used for several applications such as plastic bottles or coated papers for food and beverage packaging. Thus, PLA is an ideal candidate to prepare blends with PHB since it is a natural polymer with biodegradability and biocompatibility properties. Moreover, PHB/PLA polymer blends have shown good mechanical deformation properties [15,18,19]. So far, this polymer system has undergone extensive investigations of crystallization, miscibility and orientation behavior [20–23].

In previous research [18], FT-IR 2D imaging spectroscopy has been applied to study the miscibility of polymer blends of poly(3-hydroxybutyrate) (PHB) and poly(L-lactic acid) (PLA) as a function of the blend composition. From these investigations, the concentration dependence of phase separation at room temperature was determined. Thus, it could be shown that PHB/PLA polymer blends exhibit a miscibility gap between 50 and 60 wt.% PHB, where separation in PHB-rich and PLA-rich phases was detected. Moreover, the composition of the separated phases could be determined based on a FT-IR spectroscopic calibration in the compositional range of miscible PHB/PLA blends.

2. Experimental

2.1. Materials and sample preparation

Bacterially synthesized poly(3-hydroxybutyrate) (Sigma–Aldrich, M_w =437,000 g/mol) and poly(L-lactic acid) containing 10% meso-lactic acid (Natureworks LLC, Minnesota, USA, M_w = 240,000 g/mol) were used without further purification for the experiments. Whereas the PHB used for our experiments had at room temperature a crystallinity of >60%(w/w) the PLA had only a low crystallinity of about 30% (wt.%) because it contained 10% (wt.%) of meso-lactic acid segments. The PHB/PLA (50:50 wt.%) polymer blend was prepared by dissolving equal amounts of both polymers in chloroform. In the next step, a polymer film with a thickness of 10 μm was prepared by casting from chloroform solution on microscope slides and subsequent evaporation of the solvent at 35 °C. Finally, a small piece 2 mm (length) × 60 μm (width) × 10 μm (thickness) of such a film was mounted on a metal pin that is held within a magnetic holder. The sample was glued to the metal pin at one end of the 2 mm length, with the metal pin oriented along the central axis at the center of the 60 μm width, parallel to the edge of the film. For the projection measurements described below, the sample was thus rotated about the center axis along the length of the film, with the axis of rotation oriented perpendicular to the direction of propagation of the infrared beam. The sample was not translated in the lateral direction during data acquisition.

2.2. Measurements of synchrotron-based infrared spectro-micro-tomography

Exploiting the rapid 2D spectral image acquisition capability of IRENI enables collection of a large number of transmission images as a sample is precisely rotated [24]. Thus, recording projection images as a function of sample angle corresponds to a tomographic data set. Here, 134 projection images were collected, with an angular spacing of 2.7 degrees/step, and 50 scans were coadded for each projection image. All images were collected at one lateral position. For each wavelength, a full 3D representation of the sample can be reconstructed [24], and because we collect a full mid-IR spectrum for each data point, we can produce four-dimensional reconstructions: three spatial dimensions plus a spectral dimension. We therefore create a novel spectro-micro-tomography technique that provides not only the rich spectral information and chemical fingerprinting of FT-IR spectroscopy, but also the 3D distribution of those spectral signatures throughout the sample. This spectro-micro-tomography technique greatly enhances the capabilities of both FT-IR spectroscopy and tomography by creating a "full color" micro-tomography where colors can be assigned by specific spectral identification or spectral changes, and each voxel contains a full IR spectrum. In the present study the region of interest was a 120 μm × 60 μm × 10 μm volume and for the assignment of the PHB- and PLA-specific phases the areas of the right and left wings, respectively, of the ν(C=O) region have been used [18,22].

2.3. 3D spectro-micro tomographic reconstruction

Computed tomography is a well-established approach [25,26] used to reconstruct cross-sectional slices through an object from the transmitted projection images taken as a function of angle around a single axis of rotation. These slices can be stacked to produce a 3D image of the object, which can then be visualized by a number of methods, including volume rendering or digitally slicing through the sample along any arbitrary plane. The first demonstration of acquiring wide ranging spectral images, particularly using the power of FT-IR spectral imaging across the mid-IR fingerprint region, as a function of sample rotation angle to obtain a complete spectral tomographic data set was possible with IRENI [11]. This is feasible since high quality FT-IR spectral images are collected in about one minute with widefield (WF) spectro-microscopy, thus, acquiring a full tomographic data set requiring 100 or more spectral projection images can be obtained in a reasonable amount of time.

Reconstruction for any one wavelength image was accomplished using either filtered backprojection or iterative penalized likelihood tomographic reconstruction from the ASPIRE package [27–31]. Although not strictly correct. a parallel beam was assumed, because the beam waist created by the focus at IR wavelengths of the twelve beams (all wavelengths are 3–10 times longer than the effective pixel resolution) is approximated reasonably well by a parallel beam. Reconstruction of the transmission image of one wavelength is similar to traditional X-ray tomography.

3. Results and discussion

A 2D projection image for the PLA- and PHB-specific distributions in the PHB/PLA (50:50 wt.%) blend film is shown in Fig. 2 along with a series of spectra from individual pixels to demonstrate the contrast of the 2D projection image, and the quality of single pixel spectra. A visible projection image, and individual 3D chemical images for PLA- and PHB-specific distributions in the PHB/PLA (50:50 wt.%) blend film are shown in Fig. 3 (full movies can be provided as Supplemental Information).

The PLA- and PHB-specific chemical images are generated from the integrated intensities (for the 2D image) and back projection image (for the 2D image) for the spectral range 1770–1809 cm^{-1} (PLA) and 1674–1716 cm^{-1} (PHB) with a common baseline in the region of 1674–1809 cm^{-1}. The peak heights range up to 1.5 AU in

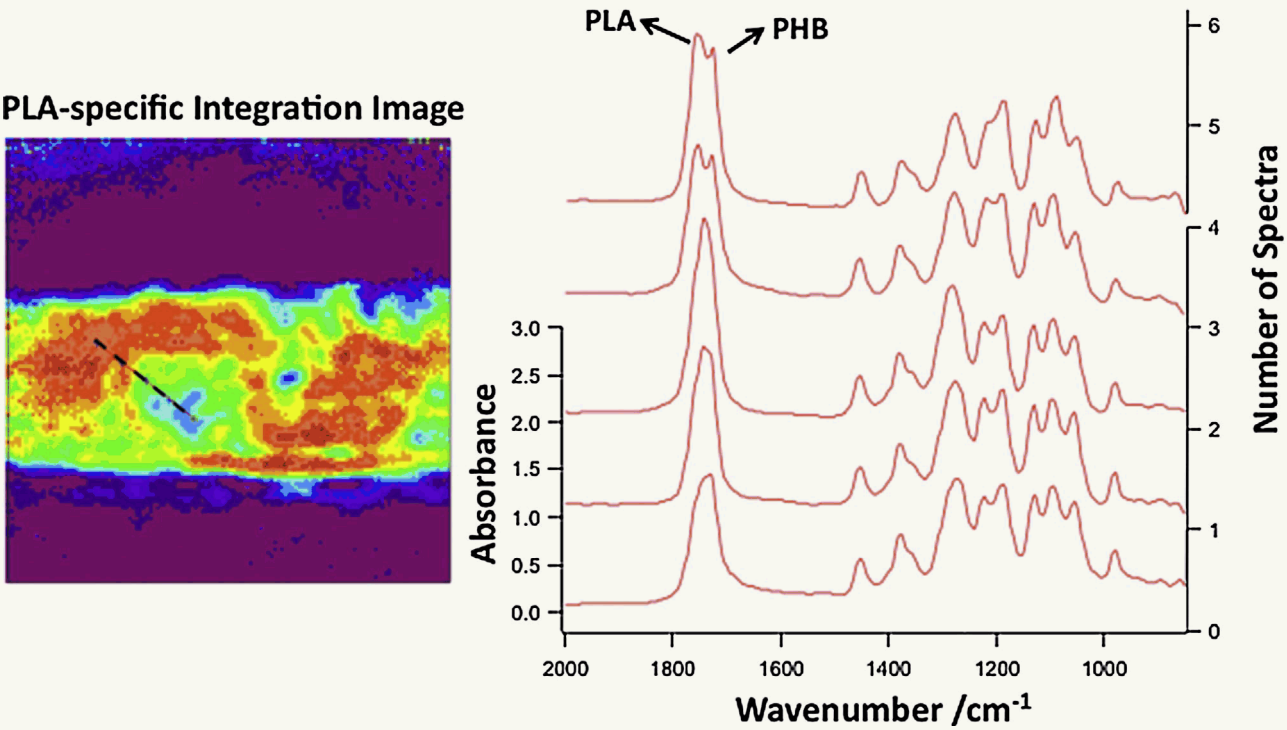

Fig. 2. 2D chemical imaging of the PHB/PLA (50:50wt%) blend film, generated from the integrated area under the PLA specific absorption band with series of spectra from single pixels along the line indicated in the 2D image. The color scale is a rainbow scale with blue (low intensity) and red (high intensity). [For interpretation of the references to color in this figure legend, the reader is referred to the web version of the article.)

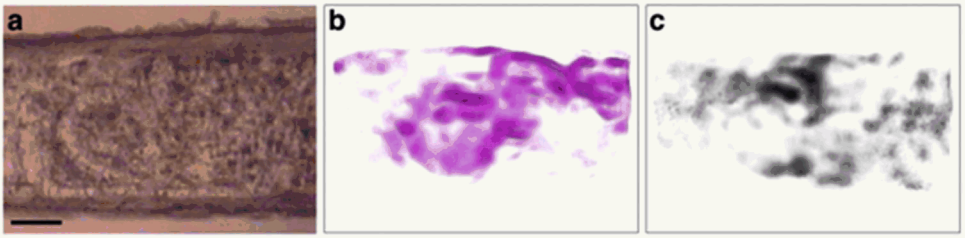

Fig. 3. 3D chemical imaging of the PHB/PLA (50:50 wt%) blend film. (a) Visible light image of the blend, the scale bar is 20 μm. Reconstruction of (b) the PHB distribution and (c) the PLA distribution in the same scale as (a). The color scale is from light (low amounts) to purple (high) for PHB and black (high) for PLA respectively. (For interpretation of the references to color in this figure legend, the reader is referred to the web version of the article.)

intensity, and are broader in the spectra extracted from the projection images corresponding to the thickest absorbing orientation. The PHB image (purple (high) to white (low) color scale), and the PLA image (black (high) to white (low) color scale) are shown from the same perspectives. It is clear that where the PLA image is at its highest intensity, there is lack of intensity in the PHB image, and vice versa. In Fig. 4, overlapping individual images from a few different vantage points highlight the separation between the two polymers.

The 3D images provide the opportunity to extract the spatial information in the *z*-direction that is lost in 2D transmission measurements, because the 2D measurements integrate all absorptions along the z-axis to generate a projection image. Under unfavorable conditions this could lead to misinterpretation of the 2D projection

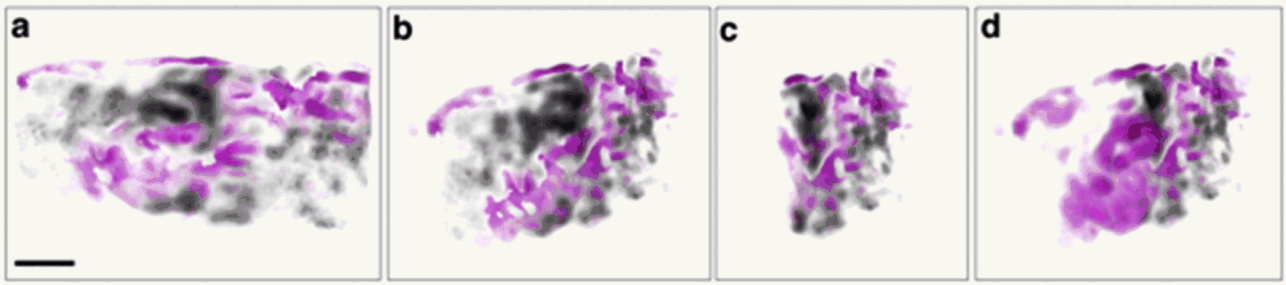

Fig. 4. Overlaying the reconstruction of PHB and PLA. In (a) the same orientation as in Fig. 3 is shown. the scale bar is 20 μm. (b)–(d)Overlay at an angle of 60° around the vertical axis. (c)Vertical cut through the sample at the center. (d) Full reconstruction image of PHB overlaid with the PLA image cut vertically at the center.

data and in the worst case could identify a phase-separated polymer as miscible. As is apparent in the 3D images, in most places as a function of *z*, both polymers are present in all projection images. That means that 2D measurements will never have truly only one polymer or another polymer contributing to any one spectrum for a given pixel. In turn, the contrast for the 2D transmission projection images will always be reduced compared to 3D renderings. The 3D results of the investigated blend system confirm that there is little overlap between the two polymers as a function of all spatial coordinates with significant distinction between the distributions of each component within the blend.This is an important factor in understanding the properties and behaviour of this novel composite polymer.

4. Conclusion

The reconstructed 3D chemical images provide information on the spatial phase distribution of the investigated PHB/PLA (50:50 wt.%) biopolymer blend film in a 120 μm × 60 μm × 10 μm volume. These 3D images confirm that the polymers are phase separated in agreement with prior miscibility studies. Future experiments will not only focus on the extraction of more detailed information regarding the quantitative composition of the phase-separated regions but will also demonstrate the application of polarized radiation for the derivation of 3D anisotropy images.

Appendix A. Supplementary data

Supplementary data associated with this article can be found, in the online version, at http://dx.doi.org/10.1016/j.vibspec.2014.07.007.

References

[1] G. Strobl, The Physics of Polymers: Concepts for understanding their Structures and Behavior, Springer, Berlin, 2007.
[2] LA. Utracki, Polymer Alloys and Blends, München. Carl Hanser Verlag, 1990.
[3] M.M. Coleman, J.F. Graf. P.C. Painter, Specific Interactions and the Miscibility of Polymer Blends, Technomic Publishing Company, Lancaster, 1991.
[4] M.M. Coleman, P.C. Painter, Appl. Spectrosc. Rev. 20 (1984) 255-346.
[5] D.R Paul, S. Newman. Polymer Blends, Academic Press, New York. 1978.
[6] R. Bhargava, S.–Q,Wang. J.L. Koenig. Adv. Polym. Sci. 163 (2003) 137-191.
[7] R. Bhargava, I.W. Levin (Eds.), Spectrochemical Analysis using Infrared Multichannel Detectors, Blackwell Publishing Ltd., Oxford, UK, 2005.
[8] R. Salzer, H.W. Siesler (Eds.). Infrared and Raman Spectroscopic Imaging. Wiley-VCH, Weinheim, 2009.
[9] S.Šašić, Y. Ozaki (Eds.). Raman, Infrared and Near-Infrared Chemical Imaging. John Wiley & Sons, Inc., Hoboken, 2010.
[10] H. Sato, Y. Ozaki, J. Jiang, R.-Q. Yu, H. Shinzawa, Vibrational spectroscopy imaging of polymers, in: S. Šašić, Y. Ozaki (Eds.). Raman, Infrared and Near-Infrared Chemical Imaging. John Wiley & Sons, Inc., Hoboken, 2010, pp. 263-281.
[11] M.J. Nasse, M.J. Walsh, E.C. Mattson, R. Reininger, A. Kajdacsy-Balla, V. Macias, R. Bhargava, C.J. Hirschmugl, Nat. Methods 8 (2011) 413-416.
[12] P.J. Hocking, R.H. Marchessault, Polyhydroxyalkanoates, in: D.L. Kaplan (Ed.), Biopolymers from Renewable Resources, Springer-Verlag, Berlin, 1998, p. 220.
[13] Y. Doi, A. Steinbuechel (Eds.). Biopolymers. Vol. 3b: Polyesters II, Wiley-VCH, Weinheim. 2001.
[14] A. Steinbuechel, B. Fuechtenbusch, Tibtech 16 (1998) 419-427.
[15] R. Auras, B. Harte, S. Selke, Macromol. Biosci. 4 (2004) 835-864.
[16] A. Steinbuechel. Y. Doi (Eds.). Biopolymers. Vol. 4, Polyesters III, Wiley-VCH. Weinheim, 2001, p. 235.
[17] http://www.natureworksllc.com/ (04.06.14).
[18] C. Vogel, E. Wessel, H.W. Siesler, Biomacromolecules 9 (2008) 523-527.
[19] C. Vogel, G.G. Hoffmann, H.W. Siesler, Vib. Spectrosc. 49 (2009) 284-287.
[20] T. Furukawa, H. Sato. H. Shinzawa, I. Noda, S. Ochiai, Anal. Sci. 23 (2007) 871-876.
[21] T. Furukawa, H. Sato, R. Murakami, J. Zhang, I. Noda. S. Ochiai. Y. Ozaki. Polymer 47 (2006) 3132-3140.
[22] C. Vogel, E. Wessel, H.W. Siesler, Macromolecules 41 (2008) 2975-2977.
[23] M. Unger, H. Sato, Y. Ozaki, D. Fischer, H.W. Siesler, Appl. Spectrosc. 67 (2013) 141-148.
[24] M.C. Martin, C. Dabat-Blondeau, M. Unger, J. Sedlmair, D. Parkinson, H.A. Bechtel, B. Illman, J.M. Castro, M. Keiluweit, D. Buschke, B. Ogle, M.J. Nasse, C.J. Hirschmugl, Nat. Methods 10 (2013) 861-864.
[25] G.T. Herman, Fundamentals of Computerized Tomography: Image Reconstruction from Projection, 2nd ed., Springer, Berlin, 2010.
[26] H. Hornich, IEEE Trans. Med. Imaging 5 (1986) 169.
[27] J.A. Fessler, E.P. Ficaro, N.H. Clinthorne, K. Lange, IEEE Trans. Med. Imaging 16 (1997) 166-175.
[28] H. Erdogan, J.A. Fessler, IEEE Trans. Med. Imaging 18 (1999) 801-814.
[29] H. Erdogan, J.A. Fessler, Phys. Med. Biol. 44 (1999) 2835-2851.
[30] J.A. Fessler, W.L. Rogers, IEEE Trans. Image Process. 5 (1996) 1346-1358.
[31] J.W. Stayman, J.A. Fessler, IEEE Trans. Med. Imaging 19 (2000) 601-615.